

Single-shot measurement of the full spatio-temporal field of ultrashort pulses with multi-spectral digital holography

Pablo Gabolde and Rick Trebino

Georgia Institute of Technology, School of Physics, 837 State St. NW Atlanta, GA 30332, USA
Pablo.Gabolde@physics.gatech.edu

Abstract: We present a remarkably simple technique for measuring the full spatio-temporal electric field of a single ultrashort laser pulse. It involves capturing a large digital hologram containing multiple smaller holograms, each of which characterizes the spatial intensity and phase distributions of an individual frequency component of the pulse. From that single camera frame, we numerically reconstruct the complete electric field, $E(x,y,t)$, using a direct algorithm. While holography requires a well-characterized reference pulse, this pulse can easily be generated from the pulse itself in most cases, so the technique is self-referencing. We experimentally demonstrate this technique using femtosecond pulses from a mode-locked Ti:Sapphire oscillator.

© 2006 Optical Society of America

OCIS Codes: (090.2880) Holographic interferometry; (320.7100) Ultrafast measurements.

References and links

1. J. P. Geindre, P. Audebert, A. Rousse, F. Fallières, J. C. Gauthier, A. Mysyrowicz, A. Dos Santos, G. Hamoniaux, and A. Antonetti, "Frequency-domain interferometer for measuring the phase and amplitude of a femtosecond pulse probing a laser-produced plasma," *Opt. Lett.* **19**, 1997-1999 (1997).
2. T. Tanabe, H. Tanabe, Y. Teramura, and F. Kannari, "Spatiotemporal measurements based on spatial spectral interferometry for ultrashort optical pulses shaped by a Fourier pulse shaper," *J. Opt. Soc. Am. B* **19**, 2795-2802 (2002). <http://www.opticsinfobase.org/abstract.cfm?URI=josab-19-11-2795>.
3. L. Gallmann, G. Steinmeyer, D. H. Sutter, T. Rupp, C. Iaconis, I. A. Walmsley, and U. Keller, "Spatially resolved amplitude and phase characterization of femtosecond optical pulses," *Opt. Lett.* **26**, 96-98 (2001). <http://www.opticsinfobase.org/abstract.cfm?URI=ol-26-2-96>.
4. C. Dorrer, E. M. Kosik, and I. A. Walmsley, "Direct space-time characterization of the electric fields of ultrashort optical pulses," *Opt. Lett.* **27**, 548-550 (2002). <http://www.opticsinfobase.org/abstract.cfm?URI=ol-27-7-548>.
5. S. A. Diddams, H. K. Eaton, A. A. Zozulya, and T. S. Clement, "Full-field characterization of femtosecond pulses after nonlinear propagation," Conference on Lasers and Electro-Optics, Paper CFF3 (1998).
6. B. C. Platt, and R. Shack, "History and Principles of Shack-Hartmann Wavefront Sensing," *J. Refractive Surg.* **17**, S573-S577 (2001).
7. J. Liang, B. Grimm, S. Goelz, and J. F. Bille, "Objective measurement of wave aberrations of the human eye with the use of a Hartmann-Shack sensor," *J. Opt. Soc. Am. A* **11**, 1949-1957 (1994). <http://www.opticsinfobase.org/abstract.cfm?URI=josaa-11-7-1949>.
8. R. G. Lane, and M. Tallon, "Wave-front reconstruction using a Shack-Hartmann sensor," *Appl. Opt.* **31**, 6902-6908 (1992).
9. E. Leith, C. Chen, Y. Chen, D. Dilworth, J. Lopez, J. Rudd, P. C. Sun, J. Valdmann, and G. Vossler, "Imaging through scattering media with holography," *J. Opt. Soc. Am. A* **9**, 1148-1153 (1992). <http://www.opticsinfobase.org/abstract.cfm?URI=josaa-9-7-1148>.
10. S. Grilli, P. Ferraro, S. De Nicola, A. Finizio, G. Pierattini, and R. Meucci, "Whole optical wavefields reconstruction by Digital Holography," *Opt. Express* **9**, 294-302 (2001).
11. S. Lai, B. King, and M. A. Neifeld, "Wave front reconstruction by means of phase-shifting digital in-line holography," *Opt. Commun.* **173**, 155-160 (2000).
12. P. Gabolde, and R. Trebino, "Self-referenced measurement of the complete electric field of ultrashort pulses," *Opt. Express* **12**, 4423-4428 (2004).

13. Z. Liu, M. Centurion, G. Panotopoulos, J. Hong, and D. Psaltis, "Holographic recording of fast events on a CCD camera," *Opt. Lett.* **27**, 22-24 (2002). <http://www.opticsinfobase.org/abstract.cfm?URI=ol-27-1-22>.
14. M. Takeda, H. Ina, and S. Kobayashi, "Fourier-transform method of fringe-pattern analysis for computer-based topography and interferometry," *J. Opt. Soc. Am.* **72**, 156-160 (1982).
15. P. H. Lissberger, and W. L. Wilcock, "Properties of All-Dielectric Interference Filters. II. Filters in Parallel Beams of Light Incident Obliquely and in Convergent Beams," *J. Opt. Soc. Am.* **29**, 126-130 (1959). <http://www.opticsinfobase.org/abstract.cfm?URI=josa-49-2-126>.
16. M. Bass, "*Handbook of Optics*, 2nd ed.," 42.89-42.90 (1995).
17. P. O'Shea, M. Kimmel, X. Gu, and R. Trebino, "Highly simplified device for ultra-short measurement," *Opt. Lett.* **26**, 932-934 (2001).

1. Introduction

The measurement of the spatial or temporal intensity-and-phase profile of ultrashort pulses is now a standard procedure in ultrafast optics laboratories. In many situations, however, separate spatial and temporal measurements are insufficient, and the measurement of the complete spatio-temporal dependence of the pulse is necessary. For example, a pulse can be contaminated by spatio-temporal distortions that limit the performance of an ultrafast system (notably in the case of amplified pulses). Or the pulse may have been used to excite or probe complex media with time-varying spatial structure. Indeed, spatio-temporal distortions are quite common, and only very carefully aligned ideal pulses/beams can be considered to be free of them.

A highly detailed, multi-dimensional pulse characterization—the (4D) field as a function of all three spatial dimensions and time, $E(x,y,z,t)$ —is thus highly desirable. But, because digital cameras and other optoelectronic sensors are obviously limited to only two dimensions, standard techniques yield at best only 2D information, $E(x,t)$ or $E(x,y)$, from a single data frame. Such techniques include linear and nonlinear spectral interferometry [1-4], sometimes combined with frequency-resolved optical gating (FROG) [5], direct wave-front sensing [6-8], and digital holography [9-11].

The complete 4D measurement problem is not hopeless, however. It is sufficient to be able to measure the 3D field, $E(x,y,t)$ at a single plane, $z = z_0$. This is because it and the Fresnel integral yield the field's dependence on the z -coordinate, too (that is, the complete 4D measurement), when propagation through free space (or known optics) is involved.

To measure the 3D electric field, $E(x,y,t)$, or equivalently, $E(x,y,\omega)$, multiple camera frames can be combined. This is usually accomplished by measuring the field vs. two of the dimensions using a camera, while scanning the remaining dimension and acquiring multiple camera frames. In fact, we recently demonstrated self-referenced multi-shot 3D measurements of the intensity and phase of the full field $E(x,y,t)$ by a combination of wavelength-scanned digital holography and FROG [12]. But, because a scan of the wavelength is required as multiple frames of data are recorded, a stable train of identical pulses is required in this type of experiment. This requirement can be prohibitive, however, especially for systems that operate at very low repetition rates or have fluctuations in the field from shot to shot.

To overcome this limitation, we introduce here a device capable of measuring the complete 3D spatio-temporal electric field $E(x,y,t)$ on a *single-shot*. Instead of recording multiple digital holograms for different wavelengths sequentially in time [12], we record them simultaneously in a larger two-dimensional camera frame. This large digital hologram contains all the necessary information to numerically reconstruct the full 3D electric field $E(x,y,t)$. For that reason, we call our technique Spatially and Temporally Resolved Intensity and Phase Evaluation Device: Full Information from a Single Hologram (STRIPED FISH).

Setups for the simultaneous recording of a few holograms have been introduced in the past, but these involve a set of beam-splitters (or a special cavity) to generate a few replicas that must all be synchronized using delay lines [13]. As a result, they do not scale very well as the pulse becomes more complex in time (or frequency) and the number of necessary holograms

increases. STRIPED FISH, on the other hand, involves a remarkably simple and elegant arrangement comprising only two main components that readily generate a large number of holograms and should, in principle, scale to complex pulses in space and/or time. Also, the multiple digital holograms may be obtained by interfering the pulse under test with a well-characterized reference pulse or, alternatively, with a spatially-filtered replica of the pulse itself whose (spatially-uniform) spectral intensity and phase are measured by FROG. Thus STRIPED FISH is self-referencing, and so should be ideal for low-repetition-rate systems.

2. Principle of operation

We first briefly recall how digital holography can be used to reconstruct the intensity and phase of the spatial electric field $E(x,y)$ of a monochromatic laser beam [10]. It involves crossing the “signal” beam (the beam to be characterized) and a “reference” beam (a pre-characterized beam) at a small angle α , in, say, the vertical plane. One then measures the corresponding intensity $I(x,y)$, or “digital hologram”, using a digital camera:

$$I(x, y) = |E_s(x, y)|^2 + |E_r(x, y)|^2 + E_s(x, y)^* E_r(x, y) e^{-iky \sin \alpha} + E_s(x, y) E_r(x, y)^* e^{iky \sin \alpha} \quad (1)$$

Because the last term of Eq. (1) contains the modulation term, $\exp(iky \sin \alpha)$, we may readily extract it from the measured intensity $I(x,y)$ using a well-established algorithm [14], which involves Fourier filtering the hologram and retaining only the last term. Assuming that we know the electric field of the reference pulse, $E_r(x,y)$, we can obtain the electric field of the signal pulse, $E_s(x,y)$, which contains both the spatial intensity (“beam profile”) and the phase (“wave-front”) of the beam.

A holographic technique generalized for broadband pulses/beams, rather than monochromatic beams, involves frequency-filtering the reference and signal pulses and generating monochromatic holograms for each frequency in the pulses. If we perform the reconstruction process at different frequencies ω_k spaced by $\delta\omega$, which satisfy the sampling theorem and which cover the bandwidth of the signal and reference pulses, we obtain the electric field $E(x,y)$ for each frequency ω_k . If the reference pulse’s spectral phase is also known, it is then easy to reconstruct the signal field in the frequency domain, which then yields the complete field in the time domain:

$$E(x, y, t) = \frac{1}{2\pi} \int E(x, y, \omega) e^{i\omega t} d\omega \simeq \frac{1}{2\pi} \sum_k E(x, y) \Big|_{\omega_k} e^{i\omega_k t} \delta\omega \quad (2)$$

In contrast to multi-shot setups that rely on a scan of the wavelength to reconstruct $E(x,y,t)$ [12], STRIPED FISH only requires a single camera frame to do so. We still cross the signal and the reference pulses at a small vertical angle, but we additionally generate multiple digital holograms on a single camera frame to obtain the complete spatial and spectral dependence of the signal pulse in a remarkably simple single-shot geometry.

The STRIPED FISH principle is illustrated in Fig. 1. It involves generating multiple holograms, one for each frequency component in the pulse and then combining them to yield $E(x,y,\omega)$. Specifically, this entails interfering the signal pulse with the pre-characterized reference pulse at a small vertical angle α (about the x -axis) as in standard holography. But then these two pulses pass through a low-resolution 2D diffraction grating, which generates a 2D array of replicas of the incident signal and reference pulses, yielding an array of holograms, all with horizontal fringes, where the beams cross. The second component of STRIPED FISH, a tilted interference band-pass filter or etalon, spectrally filters the beams into wavelengths that depend on the horizontal propagation angle [15, 16], because the band-pass filter is tilted by an angle β about the y -axis in the x - z (horizontal) plane. Finally, we also orient the 2D diffraction grating so that it is rotated slightly about the optical axis z . As a result, the hologram array is also slightly rotated, so each hologram involves pairs of beams of a (uniformly spaced) different wavelength. The resulting quasi-monochromatic holograms, each at a different color, yield the complete spatial field (intensity and phase) for each color in the

pulse and can then be combined to yield the complete spatio-temporal field of the signal pulse, $E(x,y,t)$. A single camera frame is all that is required.

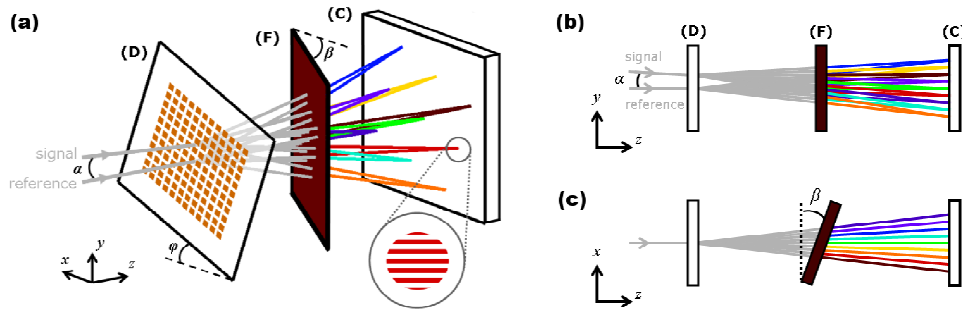


Fig. 1. Principle of operation of STRIPED FISH to measure $E(x,y,t)$. (a) View in the x - y - z space. (D): diffractive element; (F): band-pass interference filter; (C): digital camera. The signal and reference pulses are crossed at a small vertical angle α . The diffractive element (D) is rotated by an angle ϕ about the z -axis, and the filter (F) is rotated by an angle β about the y -axis. The inset shows one of the spatial interferograms (“digital holograms”) captured by the digital camera. (b) Side view (y - z plane) showing the signal and reference beams crossing at an angle. (c) Top view (x - z plane) showing how the frequencies transmitted by the band-pass filter increase with position x .

We choose the spatial period of the 2D grating to be much larger than the wavelength of the beams, so that many orders are diffracted at small and different angles. At the same time, we also choose the spatial period to be smaller than the beam spatial features that need to be resolved. As long as the bandwidth of the input beam is small compared to its central wavelength, angular dispersion within each diffracted order remains negligible.

3. Reconstruction of the electric field from a measured STRIPED FISH trace

To obtain the complex electric field $E(x,y,\omega)$, we apply the standard reconstruction algorithm to the measured STRIPED FISH trace (Fig. 2). It involves first performing a 2D Fourier transform of the STRIPED FISH trace. When the different holograms are well separated [Fig. 2(a)], the only spatial fringes that are visible are the ones due to the small vertical crossing angle α between the signal and the reference pulses. Therefore, in the Fourier domain [Fig. 2(b)], we expect to obtain one central region corresponding to the non-interferometric terms, and two other regions corresponding to the interferometric terms due to the crossing angle α . We only retain the upper region, which is the equivalent of the last term of Eq. (1), and we inverse-Fourier-transform that region to obtain a complex-valued image [Fig. 2(c)].

This image contains a collection of spectrally-resolved complex electric fields $E(x,y)$ measured at various frequencies, once we divide by the field of the reference pulse. These electric fields are distributed over the camera frame and need to be centered one by one. We use data from a reference experimental image obtained from a pulse free of spatio-temporal distortions to find the beam center corresponding to each spatial electric field, so that the data can be reorganized in a 3D data cube, $E(x,y,\omega)$. During this registration step, each digital hologram is assigned a frequency ω_k using calibrated data previously obtained by measuring the spectra of the various diffracted beams [see Fig. 2(c)].

Finally, we apply Eq. (2) to reconstruct the field $E(x,y,t)$ in the time domain. Using diffraction integrals, we can also numerically propagate the electric field through known elements along the z direction if desired to attain the full 4D spatio-temporal field.

The spatial resolution of STRIPED FISH is limited by three effects: the angular dispersion introduced by the diffractive grating, the period of the grating itself, and the size of the filtering

window in the Fourier domain. Although the 2D grating introduces some angular dispersion within each digital hologram, slightly blurring the spatial profile of the beam, a very narrow band-pass filter may be used to reduce this effect (except in the case of extremely short pulses) at the expense of a decreased throughput. The period of the diffractive element also limits the spatial resolution, although the input beam can be expanded to compensate for that effect, as long as a large-area digital camera is used. Finally, the spatial resolution can also be limited by the size of the filtered window in the Fourier plane, limiting the spatial resolution to a few pixels. In practice we are restricted by this last effect.

Similarly, the spectral resolution is also controlled by two separate factors: the bandwidth $\delta\lambda$ of the band-pass filter, and the number N of holograms that fit on the digital camera. The latter is usually the limiting factor: the spectral resolution is then simply a fraction of the pulse bandwidth $\Delta\lambda/N$, where $\Delta\lambda$ is the pulse bandwidth.

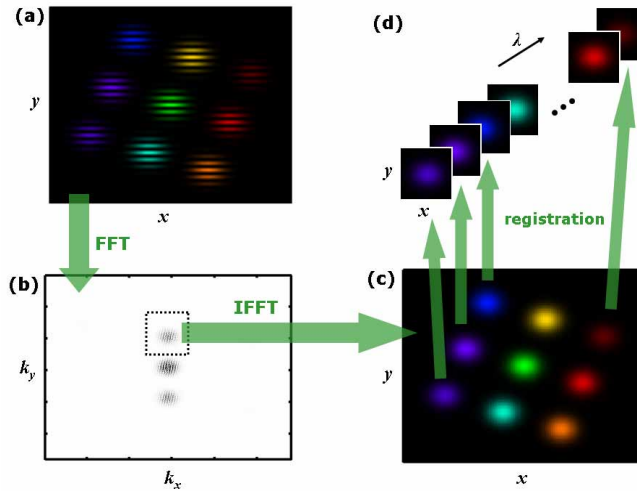


Fig. 2. Algorithm used to reconstruct the 3D electric field from a single camera frame. A 2D fast Fourier transform is applied to a simulated STRIPED FISH trace (a). The interferometric terms are selected in the Fourier plane (b), and transformed back to the original x - y plane (c). The resulting image contains both the spatial amplitude and phase, at the expense of a loss of vertical spatial resolution. A registration step is applied to center all the spatial distributions, and to assign the calibrated wavelengths, in order to obtain the multi-spectral complex data $E(x,y,\omega)$ (d).

Note that it is possible to favor the spectral resolution by using more (but smaller) holograms, which will in turn decrease the spatial resolution. Conversely, one could favor the spatial resolution using larger (but fewer) holograms. Thus, there is a trade-off between spatial and spectral resolution. We can quantify the overall performance of STRIPED FISH with regard to beam/pulse complexity: in our case the maximum *time*-bandwidth (TBP) product that we can hope to measure is roughly equal to the number of holograms that are captured. Similarly, the maximum *space*-bandwidth product (SBP) is approximately equal to the number of spatial points obtained by the reconstruction algorithm. In the end, the amount of information (number of independent data points), and therefore the maximum pulse complexity that our STRIPED FISH device can measure is estimated by introducing the *space-time-bandwidth product*, equal to $TBP \times SBP$, which is on the order of 10^5 in our case. The space-time-bandwidth product may be increased by expanding the beam to be characterized, and by using a larger-area digital camera with a higher pixel count.

4. Experimental setup and results

As a proof of principle, we set up a STRIPED FISH device as a Mach-Zehnder interferometer [Fig. 3(a)]. A first beam-splitter is used to separate an incident ultrashort pulse (800 nm) from a mode-locked Ti:Sapphire oscillator into a reference and a signal pulse. Pulses from the oscillator are routinely monitored with a single-shot FROG device [17] to ensure they are close to their transform limit. The pulse to be characterized is then obtained from the signal pulse before the two pulses are recombined at a second beam-splitter. This recombination is quasi-collinear: a small vertical angle $\alpha \sim 1^\circ$ is introduced in order to generate horizontal fringes on the digital camera, where both pulses are temporally and spatially overlapped.

Between the second beam-splitter and the digital camera, we insert the rotated coarse 2D diffraction grating and the tilted band-pass filter to generate the array of spectrally-resolved holograms. We fabricated the coarse diffraction grating by depositing an array of $10 \times 10 \mu\text{m}$ reflective chrome squares, spaced by $50 \mu\text{m}$, on the front surface of a glass substrate. This optic can be used in transmission or in reflection if dispersion from the substrate must be avoided. The interference band-pass filter has a nominal wavelength $\lambda_n = 837 \text{ nm}$ and a bandwidth (FWHM) of 3 nm, and we tilt it by an angle $\beta \sim 20^\circ$ to transmit the pulses centered at 800 nm. We typically generate an array of about 20 holograms, which are captured by a high-resolution (5-megapixel) CMOS camera. The wavelength corresponding to each interferogram is calibrated by measuring the local spectrum at that point using a fiber-coupled grating spectrometer.

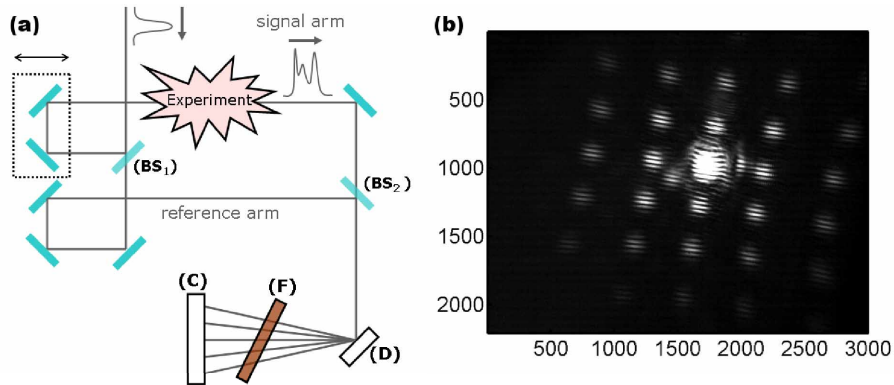


Fig. 3. (a) Mach-Zehnder interferometer used to implement our STRIPED FISH device, drawn in the x - z plane. (BS_{1,2}): beam-splitters. (D, F, C): same as in Fig. 1. The optical paths of both arms are matched using the delay stage, and a small vertical angle is introduced between the signal and reference pulses so that horizontal fringes are obtained on the digital camera. (b) Typical experimental STRIPED FISH trace (2208×3000 pixels) obtained with a 5-megapixel CMOS camera. Because of the limited dynamic range of the digital camera, the central interferogram is saturated so we discarded the corresponding data, leaving over 20 digital holograms for the data analysis.

Figure 3(b) shows a typical STRIPED FISH trace. The central interferogram, corresponding to the undiffracted order of the 2D grating, is much more intense than the other holograms. We believe this is simply due to the absence of A/R coatings on the 2D grating. Because of the limited dynamic range (10 bits) of our digital camera, we choose to saturate this region of the image and discard the data corresponding to that frequency in Eq. (2).

We demonstrate our technique using ultrashort pulses from a mode-locked Ti:Sapphire oscillator. The pulses are centered at 800 nm and have approximately 30 nm of bandwidth (FWHM). Because of the high repetition rate (80 MHz) of the laser, our measurement averages over many pulses, but our STRIPED FISH device uses a single-shot geometry, and

no scanning occurs. So it proves the principle. With a repetition rate in the kHz range and below, single-shot measurements should be straightforward.

We first show that our STRIPED FISH device is sensitive to the spectral phase of the signal pulse. We introduce some group delay in the signal pulse by delaying it with respect to the reference pulse. This modifies the absolute phase of the fringes of each digital hologram in the experimental STRIPED FISH trace. This fringe shift is recorded as a function of frequency, and as expected, a linear spectral phase is obtained [Fig. 4(a)]. Similarly, when we introduce some group-delay dispersion in the signal pulse using a dispersive window, a quadratic spectral phase is obtained [Fig. 4(b)].

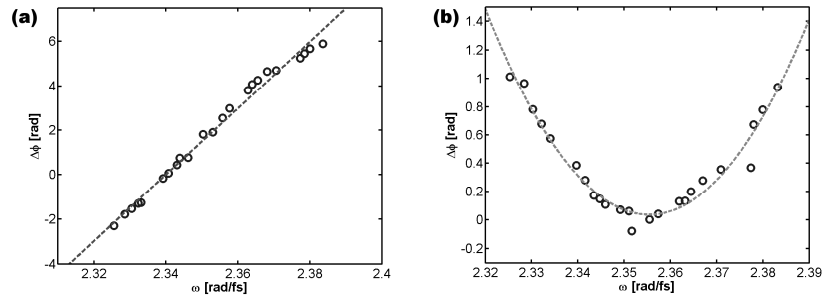


Fig. 4. (a) Fringe shift in each digital hologram as a function of frequency, showing a linear phase due to group delay. Open circles: measurement; dotted line: linear fit. (b) Fringe shift in each digital hologram as a function of frequency, showing a quadratic phase due to group-delay dispersion. Open circles: measurement; dotted line: quadratic fit.

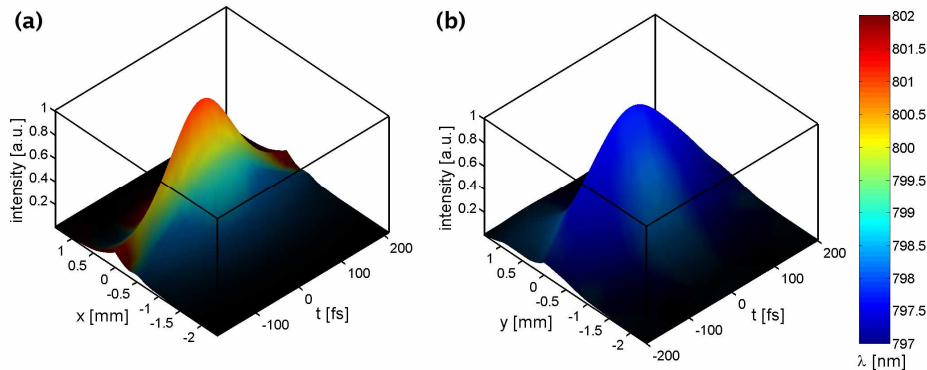


Fig. 5. (a) x - t slice of the measured electric field $E(x,y,t)$ of a pulse with spatial chirp. The vertical axis shows the electric field intensity $|E(x,t)|^2$ and the color shows the instantaneous wavelength derived from the phase $\phi(x,t)$. The spatial gradient of color shows the spatial chirp along the x direction. (b) y - t slice of the same measured electric field. No spatial chirp is present along the y direction, as expected.

We also show the reconstructed field of a pulse with horizontal spatial chirp. We introduce spatial chirp in the beam using a pair of gratings. Figure 5 shows two slices of the reconstructed electric field $E(x,y,t)$; one slice is obtained at $y = 0$ [Fig. 5(a)], and the other at $x = 0$ [Fig 5(b)]. In these plots, the instantaneous wavelength is calculated from the derivative of the temporal phase. Any temporal gradient of the instantaneous wavelength corresponds to temporal chirp, and any spatial gradient is due to spatial chirp. Horizontal spatial chirp is clearly visible on Fig 5(a).

In the aforementioned proof-of-principle experiments, the Ti:Sapphire oscillator pulse was used as the reference pulse, and a replica of that pulse was distorted in order to create an

interesting pulse for demonstration purposes [see Fig. 3(a)]. The reference pulse was therefore spatially smooth, and had an approximately flat spectral phase. However, in most cases, it should be possible to perform a full *self-referenced* measurement of the distorted signal pulse by spatially-filtering *that* pulse. The resulting pulse then has a well-defined (i.e., smooth) spatial profile, and its spectral intensity and phase may be readily characterized using a single-shot FROG device [17], so that it may be used as the reference pulse in the STRIPED FISH technique. Thus STRIPED FISH is essentially self-referencing.

5. Conclusions

We have demonstrated STRIPED FISH, a very simple, fast, and general method that can measure the complete three-dimensional spatio-temporal electric field of an ultrashort laser pulse on a single shot. It involves recording multiple holograms on a high-resolution digital camera, yielding the complete field $E(x,y,\omega)$ or $E(x,y,t)$. The complexity of the measured pulses—the space-time-bandwidth product—is a fraction of the number of pixels on the digital camera and can approach 10^5 . In the future, we hope that STRIPED FISH will allow multi-dimensional measurements of the electric field of ultrashort pulses with high resolution in space and time in a variety of important ultrashort-pulse applications.

Acknowledgments

This work was supported by NSF grant ECS-0200223 and by an endowment provided by the Georgia Research Alliance. The authors would like to thank Yuan Li and Zhibo Wu for their assistance with the fabrication of the diffractive optical element.